Lecture 34

Scattering of Electromagnetic Field

The scattering of electromagnetic field is an important topic. A source radiates a field, and ultimately, in the far field of the source, the field resembles a plane wave. When a plane wave impinges on an object or a scatterer, the energy carried by the plane wave is deflected to other directions which is the process of scattering. In the optical regime, the scattered light allows us to see objects, as well as admire all hues that are observed of objects. In microwave, the scatterers cause the loss of energy carried by a plane wave. A proper understanding of scattering theory allows us to understand many physical phenomena around us. We will begin by studying Rayleigh scattering, which is a way to study scattering by small objects.

34.1 Rayleigh Scattering

Rayleigh scattering is a solution to the scattering of light by small particles. These particles are assumed to be much smaller than wavelength of light. Then a simple solution can be found by the method of asymptotic matching. This single scattering solution can be used to explain a number of physical phenomena in nature. For instance, why the sky is blue, the sunset so magnificently beautiful, how birds and insects can navigate themselves without the help of a compass. By the same token, it can also be used to explain why the Vikings, as a seafaring people, could cross the Atlantic Ocean over to Iceland without the help of a magnetic compass.

Figure 34.1: The magnificent beauty of nature can be partly explained by Rayleigh scattering [196, 197].

When a ray of light impinges on an object, we model the incident light as a plane electromagnetic wave (see Figure 34.2). Without loss of generality, we can assume that the electromagnetic wave is polarized in the z direction and propagating in the x direction. We assume the particle to be a small spherical particle with permittivity ε_s and radius a. Essentially, the particle sees a constant field as the plane wave impinges on it. In other words, the particle feels an almost electrostatic field in the incident field.

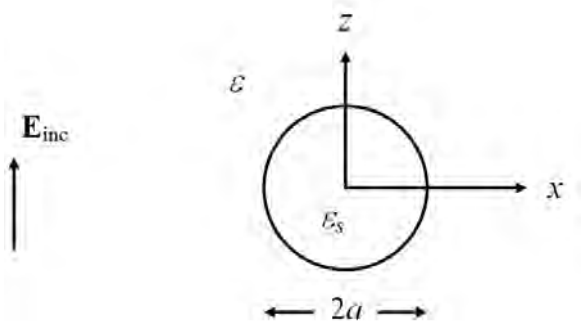

Figure 34.2: Geometry for studying the Rayleigh scattering problem.

34.1.1 Scattering by a Small Spherical Particle

The incident field polarizes the particle making it look like an electric dipole. Since the incident field is time harmonic, the small electric dipole will oscillate and radiate like a Hertzian dipole in the far field. First, we will look at the solution in the vicinity of the scatterer, namely, in the near field. Then we will motivate the form of the solution in the far field of the scatterer. (Solving a boundary value problem by looking at the solutions in two different physical regimes, and then matching the solutions together is known as asymptotic matching.)

A Hertzian dipole can be approximated by a small current source so that

$$\mathbf{J}(\mathbf{r}) = \hat{z} Il \delta(\mathbf{r}) \tag{34.1.1}$$

In the above, we can let the time-harmonic current $I = dq/dt = j\omega q$, then

$$Il = j\omega ql = j\omega p \tag{34.1.2}$$

where the dipole moment $p = ql$. The vector potential $\mathbf{A}$ due to a Hertzian dipole, after substituting (34.1.1), is

$$\begin{aligned} \mathbf{A}(\mathbf{r}) &= \frac{\mu}{4\pi} \iiint_V d\mathbf{r}' \frac{\mathbf{J}(\mathbf{r}')}{|\mathbf{r} - \mathbf{r}'|} e^{-j\beta|\mathbf{r}-\mathbf{r}'|} \\ &= \hat{z} \frac{\mu Il}{4\pi r} e^{-j\beta r} \end{aligned} \tag{34.1.3}$$

where we have made use of the sifting property of the delta function in (34.1.1) when it is substituted into the above integral.

Near Field

From prior knowledge, we know that the electric field is given by $\mathbf{E} = -j\omega\mathbf{A} - \nabla\Phi$. From dimensional analysis, the scalar potential term dominates over the vector potential term in the near field of the scatterer. Hence, we need to derive, for the corresponding scalar potential, the approximate solution.

The scalar potential $\Phi(\mathbf{r})$ is obtained from the Lorenz gauge that $\nabla \cdot \mathbf{A} = -j\omega\mu\varepsilon\Phi$. Therefore,

$$\Phi(\mathbf{r}) = \frac{-1}{j\omega\mu\varepsilon} \nabla \cdot \mathbf{A} = -\frac{Il}{j\omega\varepsilon 4\pi} \frac{\partial}{\partial z} \frac{1}{r} e^{-j\beta r} \tag{34.1.4}$$

When we are close to the dipole, by assuming that $\beta r \ll 1$, we can use a quasi-static approximation about the potential.[1] Then

$$\frac{\partial}{\partial z} \frac{1}{r} e^{-j\beta r} \approx \frac{\partial}{\partial z} \frac{1}{r} = \frac{\partial r}{\partial z} \frac{\partial}{\partial r} \frac{1}{r} = -\frac{z}{r} \frac{1}{r^2} \tag{34.1.5}$$

[1] This is the same as ignoring retardation effect.

or after using that $z/r = \cos\theta$,

$$\Phi(\mathbf{r}) \approx \frac{ql}{4\pi\varepsilon r^2}\cos\theta \tag{34.1.6}$$

which is the dipole potential. This dipole induced in the small particle is formed in response to the incident field. The scattered field from the small particle is due to a small induced dipole, and it has a potential given by the previous expression.

The incident field can be approximated by a constant local static electric field,

$$\mathbf{E}_{inc} = \hat{z}E_i \tag{34.1.7}$$

The corresponding electrostatic potential for the incident field is then[2]

$$\Phi_{inc} = -zE_i \tag{34.1.8}$$

so that $\mathbf{E}_{inc} \approx -\nabla\Phi_{inc} = \hat{z}E_i$, as $\omega \to 0$. The scattered dipole potential from the spherical particle in the vicinity of it is given by

$$\Phi_{sca} = E_s\frac{a^3}{r^2}\cos\theta = \frac{ql}{4\pi\varepsilon r^2}\cos\theta \tag{34.1.9}$$

which is the potential due to a static dipole. The electrostatic boundary value problem (BVP) has been previously solved and[3]

$$E_s = \frac{\varepsilon_s - \varepsilon}{\varepsilon_s + 2\varepsilon}E_i \tag{34.1.10}$$

Using (34.1.10) in (34.1.9), and comparing with(34.1.6), one can see that the dipole moment induced by the incident field is that

$$p = ql = 4\pi\varepsilon\frac{\varepsilon_s - \varepsilon}{\varepsilon_s + 2\varepsilon}a^3E_i \tag{34.1.11}$$

Far Field

In the far field of the Hertzian dipole, we can start with

$$\mathbf{E} = -j\omega\mathbf{A} - \nabla\Phi = -j\omega\mathbf{A} - \frac{1}{j\omega\mu\varepsilon}\nabla\nabla\cdot\mathbf{A} \tag{34.1.12}$$

But when we are in the far field, $\mathbf{A}$ behaves like a spherical wave which in turn behaves like a local plane wave if one goes far enough. Therefore, $\nabla \to -j\boldsymbol{\beta} = -j\beta\hat{r}$. Using this approximation in (34.1.12), we arrive at

$$\mathbf{E} = -j\omega\left(\mathbf{A} - \frac{\boldsymbol{\beta}\boldsymbol{\beta}}{\beta^2}\cdot\mathbf{A}\right) = -j\omega(\mathbf{A} - \hat{r}\hat{r}\cdot\mathbf{A}) = -j\omega(\hat{\theta}A_\theta + \hat{\phi}A_\phi) \tag{34.1.13}$$

where we have used $\hat{r} = \boldsymbol{\beta}/\beta$.

[2]It is not easier to get here from electrodynamics. One needs vector spherical harmonics [198].

[3]It was one of the homework problems.

34.1.2 Scattering Cross Section

From (34.1.3), and making use of (34.1.2), we see that $A_\phi = 0$ while

$$A_\theta = -\frac{j\omega\mu ql}{4\pi r} e^{-j\beta r} \sin\theta \tag{34.1.14}$$

Consequently, using (34.1.11) for ql, we have in the far field that[4]

$$E_\theta \cong -j\omega A_\theta = -\frac{\omega^2 \mu ql}{4\pi r} e^{-j\beta r} \sin\theta = -\omega^2 \mu\varepsilon \left(\frac{\varepsilon_s - \varepsilon}{\varepsilon_s + 2\varepsilon}\right) \frac{a^3}{r} E_i e^{-j\beta r} \sin\theta \tag{34.1.15}$$

$$H_\phi \cong \sqrt{\frac{\varepsilon}{\mu}} E_\theta = \frac{1}{\eta} E_\theta \tag{34.1.16}$$

where $\eta = \sqrt{\mu/\varepsilon}$. The time-averaged Poynting vector is given by $\langle \mathbf{S} \rangle = 1/2\Re e\{\mathbf{E} \times \mathbf{H}^*\}$. Therefore, the total scattered power is obtained by integrating the power density over a spherical surface when r tends to infity. Thus, the total scattered power is

$$P_s = \frac{1}{2} \int_0^\pi r^2 \sin\theta d\theta \int_0^{2\pi} d\phi E_\theta H_\phi^* = \frac{1}{2\eta} \int_0^\pi r^2 \sin\theta d\theta \int_0^{2\pi} d\phi |E_\theta|^2 \tag{34.1.17}$$

$$= \frac{1}{2\eta} \beta^4 \left|\frac{\varepsilon_s - \varepsilon}{\varepsilon_s + 2\varepsilon}\right|^2 \frac{a^6}{r^2} |E_i|^2 r^2 \left(\int_0^\pi \sin^3\theta d\theta\right) 2\pi \tag{34.1.18}$$

But

$$\int_0^\pi \sin^3\theta d\theta = -\int_0^\pi \sin^2\theta d\cos\theta = -\int_0^\pi (1 - \cos^2\theta) d\cos\theta$$

$$= -\int_1^{-1} (1 - x^2) dx = \frac{4}{3} \tag{34.1.19}$$

Therefore

$$P_s = \frac{4\pi}{3\eta} \left|\frac{\varepsilon_s - \varepsilon}{\varepsilon_s + 2\varepsilon_s}\right|^2 \beta^4 a^6 |E_i|^2 \tag{34.1.20}$$

The scattering cross section is the effective area of a scatterer such that the total scattered power is proportional to the incident power density times the scattering cross section. As such it is defined as

$$\Sigma_s = \frac{P_s}{\frac{1}{2\eta}|E_i|^2} = \frac{8\pi a^2}{3} \left|\frac{\varepsilon_s - \varepsilon}{\varepsilon_s + 2\varepsilon}\right|^2 (\beta a)^4 \tag{34.1.21}$$

In other words,

$$P_s = \langle S_{\text{inc}} \rangle \times \Sigma_s$$

[4]The ω^2 dependence of the following function implies that the radiated electric field in the far zone is proportional to the acceleration of the charges on the dipole.

It is seen that the scattering cross section grows as the fourth power of frequency since $\beta = \omega/c$. The radiated field grows as the second power because it is proportional to the acceleration of the charges on the particle. The higher the frequency, the more the scattered power. this mechanism can be used to explain why the sky is blue. It also can be used to explain why sunset has a brilliant hue of red and orange. The above also explain the brilliant glitter of gold plasmonic nano-particles as discovered by ancient Roman artisans. For gold, the medium resembles a plasma, and hence, we can have $\varepsilon_s < 0$, and the denominator can be very small.

Furthermore, since the far field scattered power density of this particle is

$$\langle S \rangle = \frac{1}{2\eta} E_\theta H_\phi^* \sim \sin^2 \theta \tag{34.1.22}$$

the scattering pattern of this small particle is not isotropic. In other words, these dipoles radiate predominantly in the broadside direction but not in their end-fire directions. Therefore, insects and sailors can use this to figure out where the sun is even in a cloudy day. In fact, it is like a rainbow: If the sun is rising or setting in the horizon, there will be a bow across the sky where the scattered field is predominantly linearly polarized.[5] Such a "sunstone" for direction finding is shown in Figure 34.3.

Figure 34.3: A sunstone can indicate the polarization of the scattered light. From that, one can deduce where the sun is located (courtesy of Wikipedia).

[5] You can go through a Gedanken experiment to convince yourself of such.

34.1.3 Small Conductive Particle

The above analysis is for a small dielectric particle. The quasi-static analysis may not be valid for when the conductivity of the particle becomes very large. For instance, for a perfect electric conductor immersed in a time varying electromagnetic field, the magnetic field in the long wavelength limit induces eddy current in PEC sphere. Hence, in addition to an electric dipole component, a PEC sphere also has a magnetic dipole component. The scattered field due to a tiny PEC sphere is a linear superposition of an electric and magnetic dipole components. These two dipolar components have electric fields that cancel precisely at certain observation angle. It gives rise to deep null in the bi-static radar scattering cross-section (RCS)[6] of a PEC sphere as illustrated in Figure 34.4.

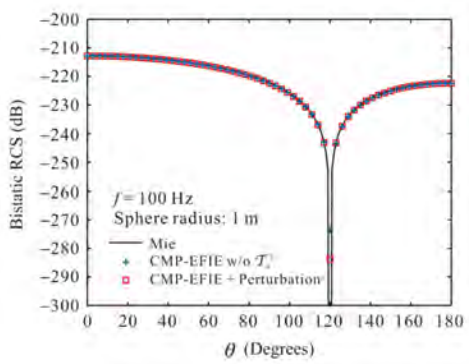

Figure 34.4: RCS (radar scattering cross section) of a small PEC scatterer (courtesy of Sheng et al. [199]).

34.2 Mie Scattering

When the size of the dipole becomes larger, quasi-static approximation is insufficient to approximate the solution. Then one has to solve the boundary value problem in its full glory usually called the full-wave theory or Mie theory [200, 201]. With this theory, the scattering cross section does not grow indefinitely with frequency as in (34.1.21). It has to saturate to a value for increasing frequency. For a sphere of radius a, the scattering cross section becomes πa^2 in the high-frequency limit. This physical feature of this plot is shown in Figure 34.5, and it also explains why the sky is not purple.

[6]Scattering cross section in microwave range is called an RCS due to its prevalent use in radar technology.

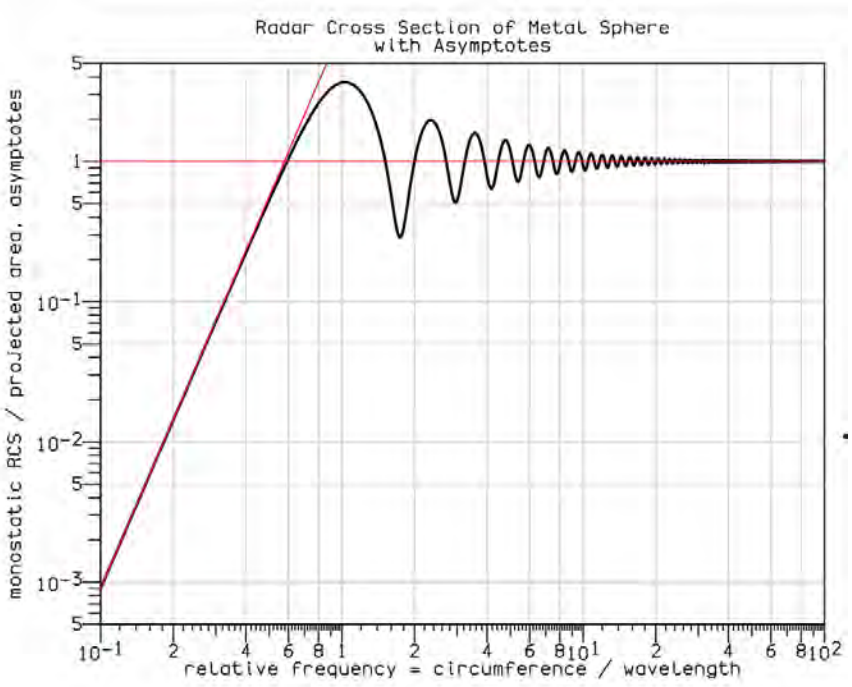

Figure 34.5: Radar cross section (RCS) calculated using Mie scattering theory [201].

34.2.1 Optical Theorem

Before we discuss the Mie scattering solution, let us discuss an amazing theorem called the optical theorem. This theorem says that the scattering cross section of a scatterer depends only on the forward scattering power density of the scatterer. In other words, if a plane wave is incident on a scatterer, the scatterer will scatter the incident power in all directions. But the total power scattered by the object is only dependent on the forward scattering power density of the object or scatterer. This amazing theorem is called the optical theorem, and the proof of this is given in J.D. Jackson's book [43].

The true physical reason for this is power orthogonality. Two plane waves cannot interact or exchange power with each other unless they share the same $\mathbf{k}$ or $\boldsymbol{\beta}$ vector, where $\boldsymbol{\beta}$ is both the plane wave direction of the incident wave as well as the forward scattered wave. This is similar to power orthogonality in a waveguide, and it happens for orthogonal modes in waveguides [76, 202].

The scattering pattern of a scatterer for increasing frequency is shown in Figure 34.6. For Rayleigh scattering where the wavelength is long, the scattered power is distributed isotropically save for the doughnut shape of the radiation pattern, namely, the $\sin^2(\theta)$ dependence. As the frequency increases, the power is scattered increasingly in the forward direction. The reason being that for very short wavelength, the scatterer looks like a disc to the incident

wave, casting a shadow in the forward direction. Hence, there has to be scattered field in the forward direction to cancel the incident wave to cast this shadow.

In a nutshell, the scattering theorem is intuitively obvious for high-frequency scattering. The amazing part about this theorem is that it is true for all frequencies.

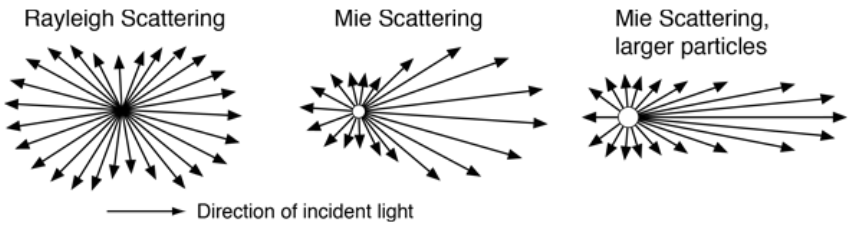

Figure 34.6: A particle scatters increasingly more in the forward direction as the frequency increases (Courtesy of hyperphysics.phy-astr.gsu.edu).

34.2.2 Mie Scattering by Spherical Harmonic Expansions

As mentioned before, as the wavelength becomes shorter, we need to solve the boundary value problem in its full glory without making any approximations. This closed form solution can be found for a sphere scattering by using separation of variables and spherical harmonic expansions that will be discussed in the section.

The Mie scattering solution by a sphere is beyond the scope of this course.[7] The separation of variables in spherical coordinates is not the only useful for Mie scattering, it is also useful for analyzing spherical cavity. So we will present the precursor knowledge so that you can read further into Mie scattering theory if you need to in the future.

34.2.3 Separation of Variables in Spherical Coordinates

To this end, we look at the scalar wave equation $(\nabla^2+\beta^2)\Psi(\mathbf{r})=0$ in spherical coordinates. A lookup table can be used to evaluate $\nabla\cdot\nabla$, or divergence of a gradient in spherical coordinates. Hence, the Helmholtz wave equation becomes[8]

$$\left(\frac{1}{r^2}\frac{\partial}{\partial r}r^2\frac{\partial}{\partial r}+\frac{1}{r^2\sin\theta}\frac{\partial}{\partial\theta}\sin\theta\frac{\partial}{\partial\theta}+\frac{1}{r^2\sin^2\theta}\frac{\partial^2}{\partial\phi^2}+\beta^2\right)\Psi(\mathbf{r})=0 \tag{34.2.1}$$

Noting the $\partial^2/\partial\phi^2$ derivative, by using separation of variables technique, we assume $\Psi(\mathbf{r})$ to be of the form

$$\Psi(\mathbf{r})=F(r,\theta)e^{jm\phi} \tag{34.2.2}$$

[7] But it is treated in J.A. Kong's book [31] and Chapter 3 of W.C. Chew, Waves and Fields in Inhomogeneous Media [34] and many other textbooks [43, 60, 167].

[8] By quirk of mathematics, it turns out that the first term on the right-hand side below can be simplified by observing that $\frac{1}{r^2}\frac{\partial}{\partial r}r^2=\frac{1}{r}\frac{\partial}{\partial r}r$.

This will simplify the $\partial/\partial\phi$ derivative in the partial differential equation since $\frac{\partial^2}{\partial\phi^2}e^{jm\phi} = -m^2e^{jm\phi}$. Then (34.2.1) becomes

$$\left(\frac{1}{r^2}\frac{\partial}{\partial r}r^2\frac{\partial}{\partial r} + \frac{1}{r^2\sin\theta}\frac{\partial}{\partial\theta}\sin\theta\frac{\partial}{\partial\theta} - \frac{m^2}{r^2\sin^2\theta} + \beta^2\right)F(r,\theta) = 0 \tag{34.2.3}$$

Again, by using the separation of variables, and letting further that

$$F(r,\theta) = b_n(\beta r)P_n^m(\cos\theta) \tag{34.2.4}$$

where we require that

$$\left\{\frac{1}{\sin\theta}\frac{d}{d\theta}\sin\theta\frac{d}{d\theta} + \left[n(n+1) - \frac{m^2}{\sin^2\theta}\right]\right\}P_n^m(\cos\theta) = 0 \tag{34.2.5}$$

when $P_n^m(\cos\theta)$ is the associate Legendre polynomial. Note that (34.2.5) is an eigenvalue problem with eigenvalue $n(n+1)$, and $|m| \leq |n|$. The value $n(n+1)$ is also known as separation constant.

Consequently, $b_n(kr)$ satisfies

$$\left[\frac{1}{r^2}\frac{d}{dr}r^2\frac{d}{dr} - \frac{n(n+1)}{r^2} + \beta^2\right]b_n(\beta r) = 0 \tag{34.2.6}$$

The above is the spherical Bessel equation where $b_n(\beta r)$ is either the spherical Bessel function $j_n(\beta r)$, spherical Neumann function $n_n(\beta r)$, or the spherical Hankel functions, $h_n^{(1)}(\beta r)$ and $h_n^{(2)}(\beta r)$. The spherical functions are related to the cylindrical functions via [34, 44] [9]

$$b_n(\beta r) = \sqrt{\frac{\pi}{2\beta r}}B_{n+\frac{1}{2}}(\beta r) \tag{34.2.7}$$

It is customary to define the spherical harmonic as [43, 203]

$$Y_{nm}(\theta,\phi) = \sqrt{\frac{2n+1}{4\pi}\frac{(n-m)!}{(n+m)!}}P_n^m(\cos\theta)e^{jm\phi} \tag{34.2.8}$$

The above is normalized such that

$$Y_{n,-m}(\theta,\phi) = (-1)^m Y_{nm}^*(\theta,\phi) \tag{34.2.9}$$

and that

$$\int_0^{2\pi}d\phi\int_0^{\pi}\sin\theta d\theta Y_{n'm'}^*(\theta,\phi)Y_{nm}(\theta,\phi) = \delta_{n'n}\delta_{m'm} \tag{34.2.10}$$

These functions are also complete[10] like Fourier series, so that

$$\sum_{n=0}^{\infty}\sum_{m=-n}^{n}Y_{nm}^*(\theta',\phi')Y_{nm}(\theta,\phi) = \delta(\phi-\phi')\delta(\cos\theta-\cos\theta') \tag{34.2.11}$$

[9] By a quirk of nature, the spherical Bessel functions needed for 3D wave equations are in fact simpler than cylindrical Bessel functions needed for 2D wave equation. One can say that 3D is real, but 2D is surreal.

[10] In a nutshell, a set of basis functions is complete in a subspace if any function in the same subspace can be expanded as a sum of these basis functions.